



## Anticancer Potential of Gold doped ZnO Nanoparticles Fabricated using Root Extract of *Kigelia africana* (Lam.) Benth. against Lung (A549), Melanoma (A375) and Epidermoid (A431) Cancer Cells

P.T.S.R.K. PRASADA RAO<sup>1,\*</sup> and N. USHA RANI<sup>2</sup>

<sup>1</sup>Department of Chemistry, P.B. Siddhartha College of Arts and Science, Vijayawada-520010, India

<sup>2</sup>Department of Freshman Engineering, P.V.P. Siddhartha Institute of Technology, Kanuru, Vijayawada-520007, India

\*Corresponding author: E-mail: ptsrkprasadrao@pbsiddhartha.ac.in

Received: 25 November 2023;

Accepted: 5 January 2024;

Published online: 28 February 2024;

AJC-21548

This study presents a simple, biocompatible and eco-friendly Au-doped ZnO nanoparticles were fabricated by employing root aqueous extract of *Kigelia africana* (Lam.) Benth. root as reducing, stabilizing and capping agent. The nanoparticles were identified by showing characteristic UV-visible wavelength maxima at 361 nm (ZnO NPs) and 569 nm (Au NPs). The nanoparticles possess polycrystalline structure with circular to oval in shape having 34 nm size that contains ~24.74 % and ~52.16 % of Au and Zn content. The FT-IR analysis confirmed the functional groups correspond to terpenoids, flavonoids and phenolics present in aqueous root extract of *Kigelia africana* (Lam.) were actively participated in nanoparticles capping. The cytotoxic applicability of fabricated nanoparticles was assessed by performing MTT assay against human lung cancer (A549) cells, melanoma cancer (A375) cells and skin or epidermoid cancer (A431) cells. The nanoparticles were proved to show potential anticancer activity with IC<sub>50</sub> concentration of 206.13 µg/mL, 152.73 µg/mL and 295.49 µg/mL against A549, A375 and A431 cell lines respectively. The IC<sub>50</sub> concentration of nanoparticles in DPPH assay was noticed as 43.75 µg/mL, whereas 33.95 µg/mL and 81.10 µg/mL respectively noticed for standard and aqueous root extract suggest that the nanoparticles possess potential antioxidant capability. Based on findings, it was suggested that the fabricated Au-doped ZnO NPs were treated as promising biocompatible candidate that can having remarkable applicability in therapeutic applications.

**Keywords:** Au-doped ZnO nanoparticles, *Kigelia africana* (Lam.) Benth., Cytotoxic studies, MTT assay, Cancer cell lines.

### INTRODUCTION

Cancer is characterized by unregulated cell growth with a high propensity to invade and metastasize surrounding cells as well as tissues through lymphatic system and bloodstream [1]. This aggressive disease claims the lives of over 10 million people annually and among the various types of cancers, lung cancer and melanoma ranking as most lethal [2]. A distinguishing feature of cancer cells, in contrast to somatic cells, is its capability to replicate and disseminate throughout the body. The release of various factors by cancer cells into their micro-environment alters the functionality of surrounding cells [3]. The mortality rate associated with lung cancer and melanoma is notably high, attributed to uncontrolled cancer cell growth in lung and skin tissues, leading to metastasis and infiltration into vital organs, such as the brain. Current cancer treatments encompass chemotherapy, hormonal therapy, immunotherapy,

radiation therapy and surgery [4]. Drawbacks of conventional chemotherapy include poor drug bioavailability in tumor tissues, high risk of potential side effects, non-specific targeting, very low therapeutic indices, requirements of high dosage and multi-drug resistance [5]. In response to these challenges, researchers have explored nanoscaled structures for their potential anti-cancer properties [6,7]. These investigations aim to overcome limitations associated with traditional chemotherapy and pave the way for more effective and targeted cancer therapies.

Therapeutic approaches involving the encapsulation of herbal compounds in nanomaterials and the targeted delivery of drugs to specific tissues have demonstrated efficacy in inducing cell death in cancer targets [8,9]. Nanoparticles have attracted significant attention in nanomedicine. Therapeutic efficacy of nanoparticles is contingent on factors such as particle size, target cell culture time, metal concentration within targeted cell and physico-chemical properties of the nanoparticles [10].

This is an open access journal, and articles are distributed under the terms of the Attribution 4.0 International (CC BY 4.0) License. This license lets others distribute, remix, tweak, and build upon your work, even commercially, as long as they credit the author for the original creation. You must give appropriate credit, provide a link to the license, and indicate if changes were made.

Additionally, bi- or multi-metallic nanoparticles exhibit distinctive physico-chemical properties characterized by synergistic effects with heightened functionality. These nanoparticles offer increased reactive sites, enhanced efficiency with enhanced stability, making them particularly intriguing for therapeutic applications [11].

Gold (Au)-zinc oxide (ZnO) bimetallic nanoparticles have garnered substantial attention in due unique properties arising from the combination of gold and zinc oxide [12]. The bimetallic nature of these nanoparticles imparts distinctive characteristics that find applications across various fields. Au-ZnO nanoparticles can be utilized in photocatalytic applications for environmental remediation and water treatment. The synergistic effects of gold and zinc oxide enhance the photocatalytic activity under light irradiation [13]. Surface of Au-ZnO nanoparticles can be functionalized to enable drug delivery that allow controlled and target release of therapeutic agents in the body. These nanoparticles show promise in cancer therapy [14]. Unique optical properties of gold nanoparticles make them suitable for photothermal therapy, while the antibacterial properties of zinc oxide contribute to enhanced therapeutic efficacy. These nanoparticles exhibit noteworthy utility in various fields, serving as effective components in gas sensors, biosensors, photovoltaic systems, light-emitting diodes, antimicrobial coatings and contributing significantly to environmental remediation [15].

*Kigelia africana* (Lam.) Benth. (sausage tree) is a medicinal plant native to sub-Saharan Africa. Its fruit, bark, leaves and roots, have been traditionally used for medicinal purposes. Scientific studies have explored the pharmacological significance of *Kigelia africana*, revealing a range of potential health benefits [16]. The literature proved that various parts such as leaf [17-19] stem [20], root [21] and fruit [22] are significantly utilized for fabrication of nanoparticles. The authors reported various pharmacological applications of the nanoparticles such as antioxidant and antibacterial activity. Further the applicability of *Kigelia africana* mediated nanoparticles as germination enhancer as well as growth promoter was reported. The elaborative literature review suggests that no author explored the anticancer applicability of nanoparticles synthesized using *Kigelia africana*. Hence this study aimed to explore the anticancer applicability of Au-doped ZnO nanoparticles fabricated using aqueous root extract of *Kigelia africana*.

## EXPERIMENTAL

**Collection of plant material:** The roots of *Kigelia africana* along with its areal parts were collected in Seshachalam Hills situated in Tirupati, India. Collection of plant was performed in agreement with international guidelines [23]. The plant specimen collected were identified by Dr. Ch. Srinivasa Reddy, Department of Botany, SRR & CVR Government Degree College, Vijayawada and issued SRR-CVR/2023/PI/01 as specimen number. The root specimens were washed carefully on a running tap water followed by distilled water for complete removal of soil particles. Then the specimen was blotted with filter paper followed by air drying to reach constant weight. Then the specimen was grinded using a mechanical grinder and the powder was preserved in an air tight amber colour bottle for further use.

**Root extract preparation:** An accurately weighed 2 g of root powder was placed in a 250 mL glass beaker contain 100 mL distilled water. The beaker was heated with moderate stirring at 70 °C in a magnetic stirrer. Then content was cooled and pure extract was collected by filtration and preserved for experimental use.

**Fabrication of Au-doped ZnO nanoparticles:** ZnO nanoparticles were fabricated by adopting procedure reported in literature [24] utilizing Zn(NO<sub>3</sub>)<sub>2</sub> as metals precursor and aqueous root extract of *K. africana* as eco-friendly reducing agent. Initially root extract was mixed 3 h followed by adding Zn metal precursor (2 g). The mixture was boiled at 60 °C till the formation of thin deposit and then it was bring to room temperature. The formed thin deposit was separated by filtration and white ZnO nanoparticles powder was collected by calcination for 1 h at 800 °C.

The Au doping on synthesized ZnO NPs surface was performed as per Fageria's procedure [24]. In brief, 10 mL of HAuCl<sub>4</sub> solution (0.01 M) was mixed with 1 % aqueous solution of synthesized ZnO NPs. To a mixture, 0.2 mL orthophosphoric acids was added, continues stirring for 4 h to generate purple deposit of Au-doped ZnO NPs and was collected by filtration, wash with distilled water and dried in an air oven. The collected Au-doped ZnO NPs were preserved in an Amber colour air tight container and the % nanoparticles yield was evaluated by using the following formula:

$$\text{Yield (\%)} = \frac{\text{Experimental weight of NPs}}{\text{Theoretical weight of NPs}} \times 100$$

**Characterization of nanoparticles:** Au-doped ZnO NPs synthesized in this study using aqueous root extract of *Kigelia africana* were characterized utilizing double-beam UV-visible spectrophotometer (JASCO International Co. Ltd., Japan) in 200-800 nm scan range for identifying and confirming the characteristic peaks corresponds to the formation of nanoparticles. Nanoparticle formation and identification of phytochemical groups were examined through Fourier transform infrared (FTIR) analysis on Bruker (USA) instrument operating within the 4000-500 cm<sup>-1</sup> range. The structural characterization of the nanoparticles was conducted through transmission electron microscopy (TEM) and energy-dispersive X-ray spectroscopy (EDX). TEM studies conducted on a Jeol JEM 2100 instrument at 120 keV. Before analysis, the nanoparticles underwent thorough washing with methanol and were subsequently affixed to carbon-coated copper grids. Crystal size and elemental composition were assessed using a Jeol 6390LA scanning electron microscopy (SEM) instrument paired with OXFORD XMx-N EDX, operating with a Tungsten lamp at an accelerating voltage of 0.5 to 30 kV. X-ray diffraction (XRD) experiment conducted on a Bruker D8 Advance EDX instrument, utilizing CuK $\alpha$  radiation. The nanoparticles underwent multiple washing with ethanol to prevent sodium chloride crystallization. The scan range for XRD analysis was set at 2 $\theta$  of 20-100°.

**Cytotoxicity or anticancer efficiency of ZnO NPs:** Cytotoxicity or anticancer efficiency of Au-doped ZnO NPs were assessed by MTT assay against human lung cancer (A549) cells, melanoma cancer (A375) cells and skin or epidermoid cancer

(A431) cells as per procedure reported by Naiel *et al.* [25]. Briefly, in a 96 wells tissue culture plate,  $1 \times 10^5$  cells/mL of selected cell lines was added at 100  $\mu\text{L}$ /well concentration separately. The plates incubated for 24 h at 37 °C. Then in each well 100  $\mu\text{L}$  of synthesized Au-doped ZnO NPs at 1, 10, 50, 100, 250 and 500  $\mu\text{g}/\text{mL}$  concentration was added. Simultaneously 4 and 8  $\mu\text{g}/\text{mL}$  concentration of doxorubicin treated as positive control and few wells kept untreated negative control for all studied cell lines. Then plates treated with nanoparticles, positive and negative control were incubated at 37 °C with 5%  $\text{CO}_2$  at 72 h. After incubation, in each well 15  $\mu\text{L}$  of MTT solution was added, incubated for 4 h and then 200  $\mu\text{L}$  of DMSO was added. Absorbance was determined at 560 nm and % survival rate was evaluated with formula:

$$\text{Survival rate (\%)} = \frac{\text{Absorbance of experimental sample}}{\text{Absorbance of control}} \times 100$$

Dose response curve was derived by plotting % inhibition *versus* concentration of sample. The Au-doped ZnO NPs require for inhibiting half the concentration of cell lines was treated as 50% cytotoxicity ( $\text{IC}_{50}$ ) concentration and was determined by adopting Probit analysis. Further, the biocompatibility of the synthesized nanoparticles was evaluated against normal cells (WI-38) in the same procedure described for cancer cell lines.

**Antioxidant activity:** DPPH (2,2-diphenyl-1-picrylhydrazyl) assay as reported by Naiel *et al.* [25] was utilized for evaluating antioxidant efficiency of Au-doped ZnO nanoparticles fabricated in this study. The procedure briefly, 1 mL of DPPH (0.1 mM in methanol) solution was mixed with 3 mL of synthesized Au-doped ZnO in concentration range of 1 to 100  $\mu\text{g}/\text{mL}$ . Simultaneously procedure was repeated by replacing nanoparticles with ascorbic acid as standard. The solutions were mixed vigorously and kept undisturbed for 30 min at room temperature. Absorbance of reaction mixture was evaluated at 517 nm against blank (without sample). The DPPH radical inhibition efficiency was evaluated using formula:

$$\text{DPPH scavenging effect (\%)} = \frac{\text{Absorbance of control} - \text{Absorbance of test}}{\text{Absorbance of control}} \times 100$$

## RESULTS AND DISCUSSION

This study targeted to fabricate Au-doped ZnO NPs utilizing active phytochemical constituents of *Kigelia africana* aqueous root extract. The pH of the reaction mixture was adjusted in pH range of 4 to 10 for producing high yield of nanoparticles with less time and based on results pH 9 was proved to be best for producing high quantity of nanoparticles that takes very less formation time than other pH values studied. The nanoparticles achieved were stable and were studied for functional and structural characterization.

Fig. 1 illustrated the optical absorption spectroscopy results of synthesized Au-doped ZnO NPs. The result clearly visualizes the presence of two absorption bands at 361 nm and 569 nm. Band at 361 nm represents and confirms ZnO NPs whereas 569 nm corresponds to Au NPs. The band at 361 nm was observed for the ZnO NPs synthesized in the study with high absorption intensity whereas the Au-doped ZnO NPs visualizes a signifi-

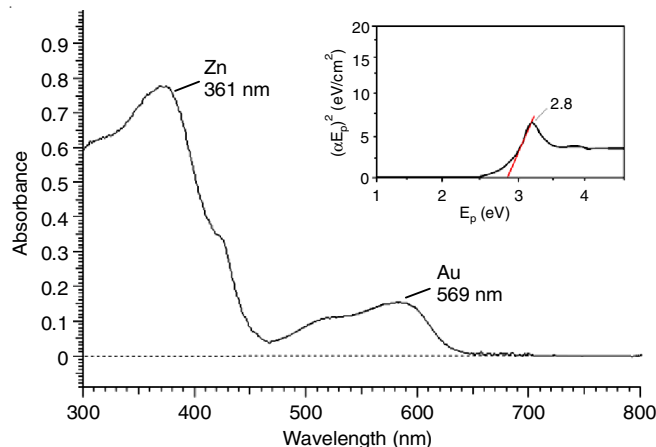


Fig. 1. UV-visible light absorption spectra of Au-doped ZnO nanoparticles. Inset visualizing the  $(\alpha E_p)^2$  against  $E_p$  plot used for calculating the band gap ( $E_g$ ) of nanoparticles

cant decrease in absorption intensity. This may be attributed due to Au presence in ZnO NPs. The UV-visible absorption results noticed for synthesized nanoparticles were in correlation with results reported in literature [26].

The absorption spectra of nanoparticles were utilized for evaluating optical band gap and were treated as factor for exhibiting interactions with biological tissues. Nanoparticles with specific band gap energies can be used for imaging, drug delivery and therapeutic applications, taking advantage of their unique optical properties. The given equation was utilized for evaluating band gap:

$$\alpha E_p = K (E_p - E_g)^{1/2}$$

In above equation,  $\alpha$  represents absorption coefficient,  $E_p$  will be discrete photo energy,  $E_g$  is band gap energy which was calculated by adopting Tauc classical approach and K is constant.

The band gap of ZnO NPs was observed to be 3.2 eV and the doing of Au reduce the band gap and exhibit a band gap of 2.8 eV. This decrease in band gap may be due to the replacement of ZnO with Au in the crystal lattice of nanoparticles. The band gap results of ZnO NPs and Au-doped NPs observed in this study were in correlation with the reported values [27,28].

The XRD carried to identify crystallinity of Au-doped ZnO NPs synthesized in this study. As represented in Fig. 2, the XRD spectrum shows reflection peaks at 31.92°, 34.37°, 36.24°, 47.50°, 56.72°, 63.01°, 67.93° and 69.18° confirmed the planes of (001), (002), (101), (102), (110), (103), (112) and (201). The polycrystalline structure of nanoparticles was confirmed by observing most pronounced peak at 36.24° (101 plane). The Scherrer's formula was applied for evaluating the crystal size (D) of nanoparticles.

$$D = \frac{K\lambda}{\beta \cos \theta} \times 100$$

where k represents constant shape factor,  $\lambda$  is the X-ray wavelength,  $\beta$  is the full width half maximum, and  $\theta$  corresponds to Bragg's angle.

Crystal size of Au-doped ZnO NPs was confirmed in 27-38 nm with 34 nm as average size. There is no additional or

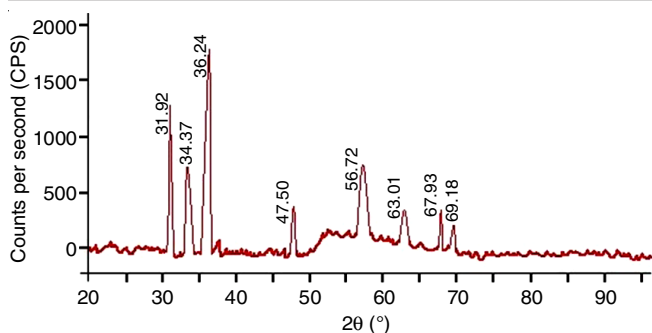


Fig. 2. XRD spectrum of Au-doped ZnO NPs fabricated with *Kigelia africana* aqueous root extract

unassigned peaks observed in XRD pattern suggest best purity of formed nanoparticles. Diffraction planes observed for the synthesized nanoparticles was in argument with the standard JCPDS card no. 36-1451 and the findings were well correlated with the literature [29].

Elemental profile of Au-doped ZnO NPs was evaluated by performing EDX studies. In EDX spectra (Fig. 3), peak corresponds to Au and Zn were detected with a % composition of ~24.74 % and ~52.16 %, respectively suggest that Zn was confirmed as major element in the formed nanoparticles. Apart from Zn, peak representing oxygen (~ 5.38) was detected and confirmed that the nanoparticles were in oxide form and peak corresponds to carbon (~ 11.52%) was detected may be due to the plant derived biomolecules involved in nanoparticles

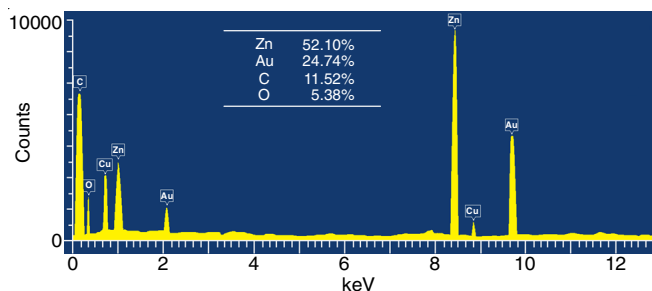


Fig. 3. EDX spectrum of Au-doped ZnO nanoparticles fabricated with *Kigelia africana* aqueous root extract

fabrication. In addition to these peaks, peaks representing Cu was detected may be due to copper grid used for EDX experiment study [30]. There is no peaks identified peaks corresponds to other elements suggest that nanoparticles were impurities free and confirms high purity.

The surface morphological features and size of Au-doped ZnO nanoparticles was evaluated using SEM and TEM analysis. The results proved that Au-doped ZnO NPs were mostly isometric in nature and less agglomerates formed during drying and hence exhibited little narrow particle size distribution. The nanoparticles were oval to spherical shape with 20-40 nm size range and average particles size was close to 34 nm. Fig. 4 represents SEM, TEM and particle size distribution results of Au-doped ZnO NPs fabricated in this study. The size of Au-doped ZnO NPs was further investigated and confirmed to be an average of 34 nm with polydispersity index (PDI) of 0.43. The zeta potential of the nanoparticles was further evaluated to prove the stability of formed nanoparticles and results suggest that nanoparticles were negatively charged with a zeta potential of -9 mV (Fig. 5). The negative charges of nanoparticles impart high stability to the particles due to the powerful repulsion in between the nanoparticles.

FT-IR experiment was conducted to identify the involvement of plant driven functional groups in the nanoparticles formation. The intense peaks identified at 3461 and 3295  $\text{cm}^{-1}$  corresponds to hydroxyl (OH) groups, which may be due to the presence of the phenolic and alcoholic compounds. The peak projected at 2911  $\text{cm}^{-1}$  represents C-H stretching group whereas the vibrational peak visualized at 1651  $\text{cm}^{-1}$  and 1551  $\text{cm}^{-1}$  were correspond to the H-O-H bending vibrations. The functional groups representing aromatic skeleton in the formed nanoparticles was proved by observing band at 2049  $\text{cm}^{-1}$  (C-H bend.), 1308  $\text{cm}^{-1}$  (C-O *str.*) and 1551  $\text{cm}^{-1}$  (C=C arom.). The identified peaks confirmed the existence of phytochemicals, including flavonoids, terpenoids and phenolics, in root extract (Fig. 6). These compounds played the substantial role in both reduction and stabilization processes of Au-doped ZnO NPs. Consistent with earlier studies, these results are corroborated by additional findings [31,32].

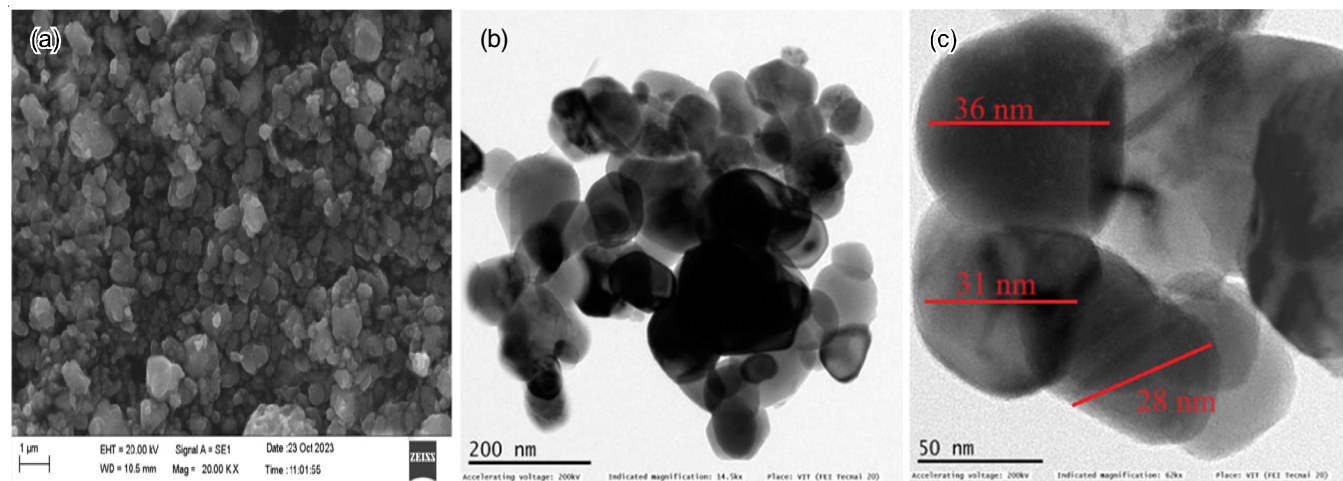


Fig. 4. Au-doped ZnO nanoparticles fabricated using aqueous root extract of *Kigelia africana* (a) SEM image and (b) TEM micrographs at two different magnification levels

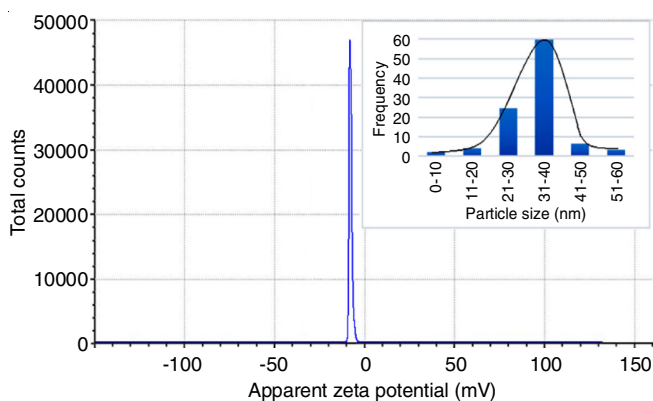
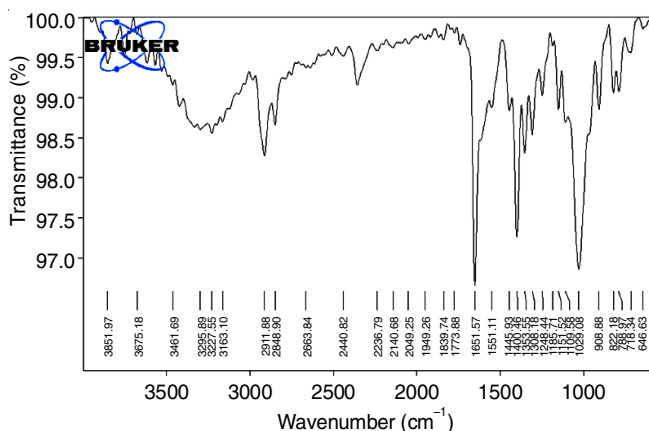
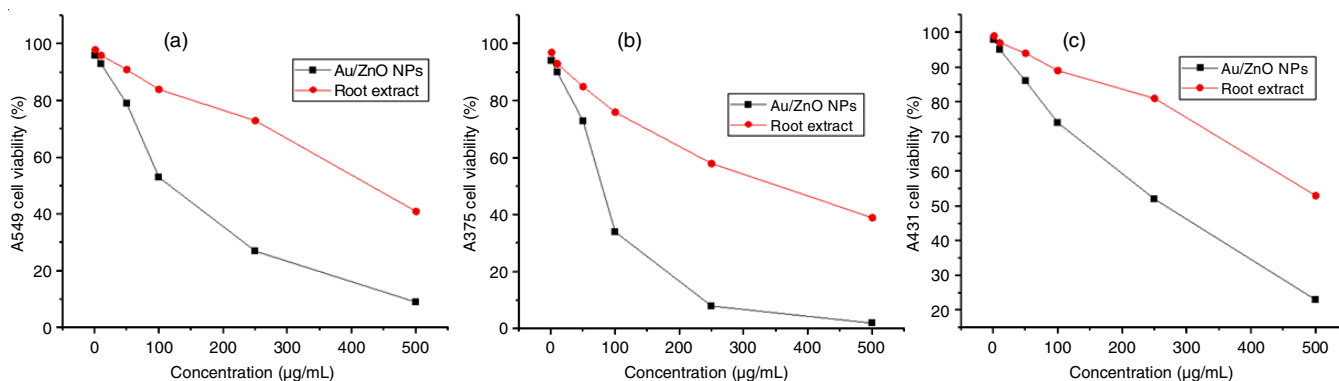


Fig. 5. Zeta potential distribution of Au-doped ZnO nanoparticles

Fig. 6. FT-IR spectrum of Au-doped ZnO nanoparticles fabricated using aqueous root extract of *Kigelia africana*

**Cytotoxicity studies:** The MTT assay was performed to evaluate the anticancer efficiency of synthesized nanoparticles against three different cell lines such as human lung cancer (A549) cells, melanoma cancer (A375) cells and skin or epidermoid cancer (A431) cells. Simultaneously the anticancer efficiency of 4 and 8  $\mu\text{g/mL}$  strength of standard doxorubicin and untreated cells was studied respectively as positive and negative control. As demonstrated in Fig. 7, nanoparticles as well as aqueous plant root extract exhibit dose dependent activity, which is in argument with finding reported previously [25,33,34].

The dose–response curve was utilized for evaluating analyte concentration of nanoparticles that inhibit cancer cell growth

Fig. 7. The % cell viability results of Au-doped ZnO nanoparticles and aqueous root extract of *Kigelia africana* against cancer cell lines against (a) lung cancer (A549) cell lines; (b) melanoma cancer (A375) cell lines and (c) skin or epidermoid cancer (A431)

to half which was designated as  $\text{IC}_{50}$  expressed in  $\mu\text{g/mL}$ . The  $\text{IC}_{50}$  concentration of 206.13  $\mu\text{g/mL}$ , 152.73  $\mu\text{g/mL}$  and 295.49  $\mu\text{g/mL}$  was achieved for A549, A375 and A431, respectively (Table-1). These nanoparticles exhibit remarkable cytotoxic potential towards melanoma cancer (A375) cells and at 500  $\mu\text{g/mL}$  concentration, the cancer cells count reached almost zero. Among the cancer cells studies, the nanoparticles exhibit high activity against melanoma cancer (A375) cells followed by lung cancer (A549) cells and epidermoid cancer (A431) cells. The  $\text{IC}_{50}$  concentration was observed to be significantly high than aqueous root extract, which was used for the fabrication of nanoparticles. This suggest that the metal at nano composition with root extract significantly enhances the cell growth inhibition and shown potential anticancer activity. Various studies also proved the potential anticancer applications of plant extracts and extract mediated nanoparticles [25,34-36], which approves the findings in this study.

TABLE-1 $\text{IC}_{50}$ CONCENTRATIONS ( $\mu\text{g/mL}$ ) NOTICED IN % CELL VIABILITY STUDY OF PHYTOSYNTHESIZED Au-DOPED ZnO NANOPARTICLES AND AQUEOUS ROOT EXTRACT OF <i>Kigelia africana</i> AGAINST CANCER CELL LINES		
Cancer cells	$\text{IC}_{50}$ concentration ( $\mu\text{g/mL}$ )	
	Au-doped ZnO NPs	Root extract
Lung cancer (A549) cells	206.13	428.68
Melanoma cancer (A375) cells	152.73	369.73
Epidermoid cancer (A431) cells	295.49	554.39

The cytotoxic effect of synthesized Au-doped ZnO nanoparticles was studied against normal cells (WI-38) for evaluating its biocompatibility. There is no inhibition of normal cell growth was observed till 250  $\mu\text{g/mL}$  concentration indicating the non-toxic ability of nanoparticles against normal cells. The normal cells have the ability to fight against reactive oxygen species (ROS) that originate from the external source. Various studies reveals that at relatively low concentration ROS are non-toxic to normal cells as well as erythrocytes [37] and statement was in argument with this study results.

The anticancer activity of Au-doped ZnO NPs involves a multifaceted mechanism that capitalizes on the unique properties of both gold and zinc. The presence of Zn in nanoparticles can lead to ROS generation within cancer cells. The elevated

levels of ROS can induce oxidative stress, damaging cellular components and triggering apoptotic pathways [25,34].

**Antioxidant activity:** Antioxidant profile of Au-doped ZnO NPs was evaluated by performing DPPH radical scavenging assay. As presented in Fig. 8, the synthesized nanoparticles shows remarkable scavenging than aqueous root extract. The dose dependent scavenging activity was observed in concentration range of 1 to 100  $\mu\text{g/mL}$ . Highest DPPH radical inhibition of 83.69 % was recorded for synthesized nanoparticles at 100  $\mu\text{g/mL}$ , which was close to standard (93.18 %) and significantly high than aqueous root extract (58.46 %). The  $\text{IC}_{50}$  concentration was found to be 43.75  $\mu\text{g/mL}$  for synthesized nanoparticles whereas the  $\text{IC}_{50}$  concentration of 33.95  $\mu\text{g/mL}$  and 81.10  $\mu\text{g/mL}$  was recorded for standard and aqueous root extract, respectively. These results suggest that Au-doped ZnO NPs exhibit significantly enhanced antioxidant activity.

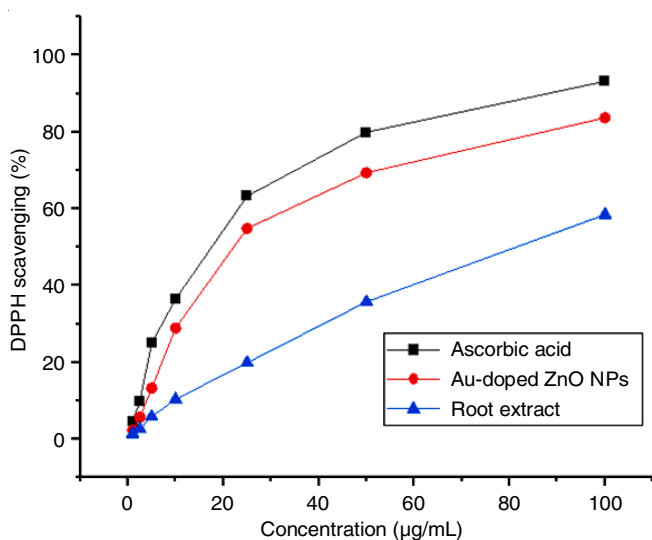


Fig. 8. DPPH radical scavenging activity of Au-doped ZnO nanoparticles in comparison with aqueous root extract of *Kigelia africana* and standard ascorbic acid

**Mechanism:** The fabrication and enhanced pharmacological activities of nanoparticles involves a complex and multifaceted mechanism that dependent on bioactive constituents. The phytochemicals such as polyphenols, flavonoids, terpenoids and alkaloids are extracted from the roots of *Kigelia africana*. These compounds possess functional groups that can serve as reducing and capping agents in nanoparticles formation. These phytochemicals facilitates the reduction of Zn metal ions to zero-valent metallic state by transferring electrons from bioactive compounds to the metal ions. The reduced Zn atoms undergo nucleation, forming the initial nuclei of nanoparticles [38,39]. As the reaction progresses, these nuclei grow into larger nanoparticles. The doping of Au facilitates formation of Au-doped ZnO NPs [40].

## Conclusion

This study demonstrated an effective application of aqueous root extract of *Kigelia africana* as reducing, capping and stabilizing agent for fabrication of Au-doped ZnO NPs. The Au-doped ZnO NPs was formed due to involvement of phenolics, flavo-

noids and terpenoids from the aqueous root extract of *Kigelia africana*. Root extract and extract mediated Au-doped ZnO NPs were studied for its cytotoxic ability against three different cancer cells such as lung (A549), melanoma (A375) and epidermoid (A431). The dose dependent cancer cell growth inhibition was observed for synthesized nanoparticles against cell lines with  $\text{IC}_{50}$  concentration of 206.13, 152.73 and 295.49  $\mu\text{g/mL}$  was achieved for A549, A375 and A431, respectively. These nanoparticles exhibit remarkable cytotoxic potential towards melanoma cancer (A375) cells. The  $\text{IC}_{50}$  concentration in DPPH radical scavenging activity was calculate to be 43.75  $\mu\text{g/mL}$ , 33.95  $\mu\text{g/mL}$  and 81.10  $\mu\text{g/mL}$  for Au-doped ZnO NPs, standard ascorbic acid and aqueous root extract respectively suggest that the nanoparticles have remarkable antioxidant efficiency. Ths, it was concluded that the Au-doped ZnO NPs fabricated with aqueous root extract of *K. africana* as cost effective and eco-friendly alternative in the biomedical applications.

## CONFLICT OF INTEREST

The authors declare that there is no conflict of interests regarding the publication of this article.

## REFERENCES

- G. Jamalipour Soufi, P. Irvani, A. Hekmatnia, E. Mostafavi, M. Khatami, S. Irvani *Comments Inorganic Chem*, 41(6), 1 (2021); <https://doi.org/10.1080/02603594.2021.1990890>
- C.S. Dela Cruz, L.T. Tanoue and R.A. Matthey, *Clin. Chest Med.*, **32**, 605 (2011); <https://doi.org/10.1016/j.ccm.2011.09.001>
- K.P. Traves and S.E. Cokenakes, *Am. Fam. Physician*, **104**, 171 (2012).
- M. Haghghat, H.Q. Alijani, M. Ghasemi, S. Khosravi, F. Borhani, F. Sharifi, S. Irvani, K. Najafi and M. Khatami, *Bioprocess Biosyst. Eng.*, **45**, 97 (2022); <https://doi.org/10.1007/s00449-021-02643-2>
- A. Sartaj, S. Baboota and J. Ali, *Curr. Pharm. Des.*, **27**, 4630 (2021); <https://doi.org/10.2174/1381612827666210902155752>
- Y. Wang and F. Wang, *Front. Pharmacol.*, **12**, 1434 (2021); <https://doi.org/10.3389/fphar.2021.685011>
- M. Barani, M. Reza Hajinezhad, S. Sargazi, M. Zeeshan, A. Rahdar, S. Pandey, M. Khatami and F. Zargari, *Polymers*, **13**, 3153 (2021); <https://doi.org/10.3390/polym13183153>
- X. Ji, Y. Cheng, J. Tian, S. Zhang, Y. Jing and M. Shi, *Chem. Biol. Technol. Agric.*, **8**, 54 (2021); <https://doi.org/10.1186/s40538-021-00255-2>
- H.Q. Alijani, S. Irvani, S. Pourseyedi, M. Torkzadeh-Mahani, M. Barani and M. Khatami, *Sci. Rep.*, **11**, 17431 (2021); <https://doi.org/10.1038/s41598-021-96918-z>
- M. Barani, M. Mirzaei, M. Torkzadeh-Mahani, A. Lohrasbi-Nejad and M.H. Nematollahi, *Mater. Sci. Eng. C*, **113**, 110975 (2020); <https://doi.org/10.1016/j.msec.2020.110975>
- R. Reshmy, E. Philip, R. Sirohi, A. Tarafdar, K.B. Arun, A. Madhavan, P. Binod, M.K. Awasthi, S. Varjani, G. Szakacs and R. Sindhu, *Bioresour. Technol.*, **337**, 125491 (2021); <https://doi.org/10.1016/j.biortech.2021.125491>
- M. Szymanski and R. Dobrucka, *J. Inorg. Organomet. Polym. Mater.*, **32**, 1354 (2022); <https://doi.org/10.1007/s10904-021-02188-7>
- S.S. Kanakillam, B. Krishnan, R.F. Cienfuegos-Peláez, J.A. Aguilar Martinez, D.A. Avellaneda and S. Shaji, *Surf. Interfaces*, **27**, 101561 (2021); <https://doi.org/10.1016/j.surfin.2021.101561>
- M. Alhujaily, M.S. Jabir, U.M. Nayef, T.M. Rashid, G.M. Sulaiman, K.A.A.A. Khalil, M.I. Rahmah, M.A.A.A. Najm, R. Jabbar and S.F. Jawad, *Metals*, **13**, 735 (2023); <https://doi.org/10.3390/met13040735>

15. S.M. Abd El-Aziz, A.A. Sleem and M.I.A. Abdel Maksoud, *Cellulose*, **30**, 303 (2023); <https://doi.org/10.1007/s10570-022-04878-y>
16. A. Nabatanzi, S.M. Nkdimeng, N. Lall, J.D. Kabasa and L.J. McGaw, *Plants*, **9**, 753 (2020); <https://doi.org/10.3390/plants9060753>
17. B. Biyela and V. Mohanlall, *Indian J. Biochem. Biophys.*, **59**, 94 (2022).
18. M. Sengani, S. Chakraborty, M.P. Balaji, R. Govindasamy, T.A. Alahmadi, S. Al Obaid, I. Karuppusamy, N.T.L. Chi, K. Brindhadevi and V. Devi Rajeswari, *Environ. Res.*, **216**, 114475 (2023); <https://doi.org/10.1016/j.envres.2022.114475>
19. N. Usha Rani, P. Pavani and P.T.S.R.K. Prasad Rao, *Asian J. Chem.*, **34**, 409 (2022); <https://doi.org/10.14233/ajchem.2022.23563>
20. C.M. Kurmarayuni, B. Chandu, L.P. Yangalasetty, S.J. Gali, B.M.K. Khandapu and H.B. Bollikolla, *ChemSelect*, **6**, 11832 (2021); <https://doi.org/10.1002/slct.202103236>
21. N. Usha Rani, P. Pavani and P.T.S.R.K. Prasad Rao, *Indian Drugs*, **59**, 34 (2022); <https://doi.org/10.53879/id.59.04.13009>
22. P.B. Ashishie, C.A. Anyama, A.A. Ayi, C.O. Oseghale, E.T. Adesuji and A.H. Labulo, *J. Nanomed. Nanotechnol.*, **13**, 24 (2018); <https://doi.org/10.5897/IJPS2017.4689>
23. International Union for Conservation of Nature, International Union for Conservation of Nature Natural Resources IUCN Red List Categories and Criteria, IUCN, Gland and Cambridge (2001).
24. P.A. Luque, C.A. Soto-Robles and O. Nava, *J. Mater. Sci.: Mater. Electron*, **29**, 9764 (2018); <https://doi.org/10.1007/s10854-018-9015-2>
25. B. Naiel, M. Fawzy, M.W.A. Halmy and A. El-Din Mahmoud, *Sci. Rep.*, **12**, 20370 (2022); <https://doi.org/10.1038/s41598-022-24805-2>
26. P. Fageria, *Rsc Adv.*, **4**, 24962 (2014); <https://doi.org/10.1039/C4RA03158J>
27. M. Julita, M. Shiddiq and M. Khair, *Indon. J. Chem. Res.*, **10**, 83 (2022); <https://doi.org/10.30598/ijcr.2022.10-mar>
28. S.M. Mishra and B. Satpati, *J. Lumin.*, **246**, 118813 (2022); <https://doi.org/10.1016/j.jlumin.2022.118813>
29. H. Zhang, D. Yang, Y. Ji, X. Ma, J. Xu and D. Que, *J. Phys. Chem. B*, **108**, 3955 (2004); <https://doi.org/10.1021/jp036826f>
30. A. Mezni, A. Mlayah, V. Serin and L.S. Smiri, *Mater. Chem. Phys.*, **147**, 496 (2014); <https://doi.org/10.1016/j.matchemphys.2014.05.022>
31. S.C. Chabattula, P.K. Gupta, S.K. Tripathi, R. Gahtori, P. Padhi, K. Dua, S. Mahapatra, B.K. Biswal, S.K. Singh, J. Ruokolainen, Y.K. Mishra, N.K. Jha, D.K. Bishi and K.K. Kesari, *Mater. Today Chem.*, **22**, 100618 (2021); <https://doi.org/10.1016/j.mtchem.2021.100618>
32. K. Dulta, G. Kosarsoy Agçeli, P. Chauhan, R. Jasrotia and P.K. Chauhan, *J. Inorg. Organomet. Polym. Mater.*, **31**, 180 (2021); <https://doi.org/10.1007/s10904-020-01684-6>
33. M. Chelladurai, R. Sahadevan, G. Margavelu, S. Vijayakumar, Z.I. González-Sánchez, K. Vijayan and K.C. Dharani Balaji, *J. Drug Deliv. Sci. Technol.*, **61**, 102180 (2021); <https://doi.org/10.1016/j.jddst.2020.102180>
34. Y. Cao, H.A. Dhahad and M.A. El-Shorbagy, *Sci. Rep.*, **11**, 23479 (2021); <https://doi.org/10.1038/s41598-021-02937-1>
35. A. Miri, M. Khatami, O. Ebrahimi and M. Sarani, *Green Chem. Lett. Rev.*, **13**, 27 (2020); <https://doi.org/10.1080/17518253.2020.1717005>
36. J. Iqbal, B.A. Abbasi, T. Yaseen, S.A. Zahra, A. Shahbaz, S.A. Shah, S. Uddin, X. Ma, B. Raouf, S. Kanwal, W. Amin, T. Mahmood, H.A. El-Serehy and P. Ahmad, *Sci. Rep.*, **11**, 20988 (2021); <https://doi.org/10.1038/s41598-021-99839-z>
37. M. Prach, V. Stone and L. Proudfoot, *Toxicol. Appl. Pharmacol.*, **266**, 19 (2013); <https://doi.org/10.1016/j.taap.2012.10.020>
38. P.P. Mahamuni, P.M. Patil, M.J. Dhanavade, M.V. Badiger, P.G. Shadija, A.C. Lokhande and R.A. Bohara, *Biochem. Biophys. Rep.*, **17**, 71 (2018); <https://doi.org/10.1016/j.bbrep.2018.11.007>
39. N. Usha Rani, P. Peddi, S. Lakshmi Tulasi and P.T.S.R.K. Prasada Rao, *Asian J. Chem.*, **35**, 923 (2023); <https://doi.org/10.14233/ajchem.2023.26938>
40. M. Carofigliio, S. Barui, V. Cauda and M. Laurenti, *Appl. Sci.*, **10**, 5194 (2020); <https://doi.org/10.3390/app10155194>